A Linear Dynamic Model for a power-recycled Michelson interferometer with Fabry-Perot arms

C.Mehmel[a]*, B.Caron[a], A.Dominjon[b], C.Drezen[b], R.Flaminio[b], X.Grave[b], R.Hermel[b], F.Marion[b], L.Massonnet[b], R.Morand[b], B.Mours[b], V.Sannibale[b], M.Yvert[b]

[a] LAMII, BP 806,F-74016 Annecy CEDEX, France

[b] LAPP, BP 110, F-74941 Annecy-le-Vieux CEDEX, France

Abstract

Large-scale gravitational-wave detectors like VIRGO or LIGO are currently under construction. These Michelson interferometers use multiple optical cavities with kilometer-scale arms lengths and therefore with long storage time.
A knowledge of the dynamic response of the interferometer is needed in order to operate it. In this study we derive a linear dynamic model for the interferometer starting by the case of a single Fabry-Perot cavity. We finally compute the interferometer transfer functions which show dynamic effects even at low frequencies.

1 Introduction

Several gravitational wave detectors based on Michelson interferometers using long Fabry-Perot cavities are under construction[1, 2]. The mirrors making up the interferometer will be suspended masses oscillating around their equilibrium points at very low frequency with an amplitude exceeding by as much as six orders of magnitude the required stability on the distances between the mirrors for the interferometer to be operational. A complex control system is therefore needed to reduce the amplitude of the mirror oscillations in order to meet the various conditions of resonance and interference defining the working point. This control system will be based on light signals collected by several photodiodes located at various places in the interferometer[3]. This paper adresses the issue of the frequency dependence of these relationships. A good knowledge of the interferometer dynamic response to movements of its mirrors is not only necessary to design the control system but will be also essential to extract the gravitational wave signal from the signals collected at the output of the interferometer. The study reported here was performed within the VIRGO framework.
We begin in section two with the simple case of a Fabry-Perot cavity illuminated with phase

*Main author to whom all correspondance should be adressed

modulated light and derive the transfer functions between the demodulated signals collected in reflection and the cavity length variations. Section three is then devoted to the more complex case of a recycled interferometer with Fabry-Perot arms. The transfer functions - obtained following the same method as that exposed in section two - between the photodiode signals of interest to the control system and the characteristic distance variations of the interferometer are given for a given set of parameters. Some of the obtained transfer functions show a strong frequency dependence of the collected signals even at low frequency and we end up by giving an interpretation for this kind of behavior.

2 Fabry-Perot Cavity Frequential Model

2.1 Field Variation Model

A Fabry-Perot cavity (fig 1) is composed by two mirrors: a front mirror and a back mirror. Each mirror is characterized by its optical parameters p_i, r_i and t_i where p_i represents the mirror losses, r_i is the mirror reflection factor and t_i denotes the mirror transmission factor. Assuming that the cavity front mirror is illuminated with a laser light, let A be the incident field amplitude, B refers to the cavity recycled field amplitude, C denotes the cavity reflected field amplitude and D denotes the amplitude of the field coming back to the front mirror. The round trip time of the cavity is given by $\tau = 2\,\frac{L}{c}$, where L is the cavity length and c represents the light velocity.

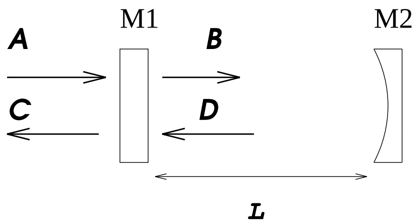

Figure 1: *Fabry-Perot cavity*

According to the figure (1), if we assume some small displacements of the cavity mirrors the equations of the field amplitudes are given by

$$\begin{aligned} C(t) &= t_1 D(t) + j\ r_1 A(t) \\ B(t) &= t_1 A(t) + j\ r_1 D(t) \\ D(t) &= \frac{1}{j\ r_1}\psi(t) B(t-\tau) \end{aligned} \tag{1}$$

With:

$$\psi(t) = \pm r_1 r_2 \exp\{j\frac{2\pi}{\lambda}\{-x_1(t-\tau) + 2x_2(t-\frac{\tau}{2}) - x_1(t) \tag{2}$$

In the above equation λ denotes the laser light wave-length. The mirrors displacements are referred to respectively by $x_1(t)$ and $x_2(t)$. Notice that if the cavity is resonant for the light frequency, the relation 2 is given with a (+) sign which means that the field coming back to the

front mirror interferes constructively with the incident field. On the other hand the relation (2) is given with a $(-)$ sign if the cavity is anti-resonant regarding to the laser light.
In the continuation of this paper we will note $\bar{R} = \pm r_1 r_2$ according to whether the cavity is resonant or anti-resonant.

Let us write each field of the figure (1) as a constant part plus a small time dependent part:

$$\chi(t) = \chi_0 + \delta\chi(t) \tag{3}$$

One can see the constant part as the steady state field value and the small part as a variation resulting from some fluctuations either in the incident field amplitude or in the mirror positions.

Assuming that the variations considered here are very small and expanding the second relation of (1) at first order leads to:

$$\delta B(t) = t_1 \delta A(t) - \bar{R}\delta B(t-\tau) - j\bar{R}\frac{2\pi}{\lambda}B_0\{-x_1(t-\tau) + 2x_2(t-\frac{\tau}{2}) - x_1(t)\} \tag{4}$$

The stationary value of the recycled field in the equation (4) is given by:

$$B_0 = A_0 \frac{t_1}{1+\bar{R}} \tag{5}$$

Notice that the equation (4) is linear, hence it can be transformed in the Laplace domain as:

$$\begin{aligned} \delta B(s) \quad = \quad & \frac{t_1}{1+\bar{R}\exp(-\tau s)}\delta A(s) \; + \; j\frac{2\pi}{\lambda}B_0 \; \bar{R}\frac{1+\exp(-\tau s)}{1+\bar{R}\exp(-\tau s)}x_1(s) \\ & - \; 2j\frac{2\pi}{\lambda}B_0 \; \bar{R}\frac{\exp(-\frac{\tau}{2}s)}{1+\bar{R}\exp(-\tau s)}x_2(s) \end{aligned} \tag{6}$$

In the above equation the quantity $\xi(s)$ denotes the Laplace transform of the temporal variable $\xi(t)$. The relation (6) gives a model for the recycled field variation. Hence the cavity can be represented by three complex transfer functions giving the relation between the recycled field variation and either the fluctuations of the incident field amplitude or the mirror displacements. One can see that the transfer functions of (6) contain the time delay term $\exp(-s\tau)$. Hence the cavity can be viewed as a sampled data system with a sample time equal to the cavity round trip time. The idea of approximating this term in order to obtain a continuous model for the inteferometer was proposed in[4], a strong motivation for such approximation is that the overall system becomes more tractable from the point of view of analysis and control design. We propose here to use the Pade first order approximation[5, 6, 7]:

$$\exp(-s\tau) \approx \frac{1-\frac{\tau}{2}s}{1+\frac{\tau}{2}s} \tag{7}$$

One can see that the two terms of (7) have the same amplitude, hence the error induced by this approximation is due to the phase error. Nevertheless given the small value of cavity round trip time this error is negligible at low frequency. Using the approximation of (7) and neglecting the second order terms in τ leads to:

$$\delta B(s) = \frac{t_1}{1+\bar{R}} \frac{1+\frac{\tau}{2}s}{1+\frac{1-\bar{R}}{1+\bar{R}}\frac{\tau}{2}s} \delta A(s) - 4j\frac{\pi}{\lambda}\frac{\bar{R}}{1+\bar{R}}\frac{1}{1+\frac{1-\bar{R}}{1+\bar{R}}\frac{\tau}{2}s}\delta L(s) \tag{8}$$

Where $\delta L = x_1 - x_2$ represents the cavity length variation.

The equation (8) gives a dynamic relation between the recycled field amplitude variation and both the incident field amplitude variation and the cavity length variation.

2.2 Power Variation Model

We will consider in this section that the laser light is phase-modulated. Hence the cavity incident field is given by:

$$A(t) = [A_0 + A_+ \exp(j\Omega t) + A_- \exp(-j\Omega t)]\exp(j\omega t) \tag{9}$$

In the relation (9) ω and Ω refer respectively to the carrier frequency and the modulation frequency. The carrier and the side-bands are given by A_0, A_+ and A_-.
Let us now consider the reflected field variation due to some small displacements of the cavity mirrors. Using the relations of (1) and (8) leads to

$$G(s) = \frac{\delta C(s)}{\delta L(s)} = -2\frac{t_1^2}{r_1}\frac{\omega}{c}A_0\frac{\bar{R}}{(1+\bar{R})^2}\frac{1}{1+\bar{\tau}s} \tag{10}$$

With $\bar{\tau} = \frac{1-\bar{R}}{1+\bar{R}}\frac{\tau}{2}$

The equation (10) gives the complex transfer function which relates the reflected field amplitude variation to the cavity length variation.

Assuming some small change of the cavity length, the power at the output of the cavity is given by:

$$\begin{aligned} P(t) = |(C_0 + \delta C_0(t)) &+ (C_+ + \delta C_+(t)) \exp(I\Omega t) \\ &+ (C_- + \delta C_-(t)) \exp(-I\Omega t)|^2 \end{aligned} \tag{11}$$

The first order approximation of the power variation can be written as:

$$\begin{aligned} \delta P(t) &= 2Re(C_0^*\delta C_0(t) + C_+^*\delta C_+(t) + C_-^*\delta C_-(t)) \\ &+ 2Re(C_0^*(\delta C_+(t) + \delta C_-(t)) + (C_+^* + C_-^*)\delta C_0(t))cos(\Omega t) \\ &+ 2Im(C_0^*(\delta C_-(t) - \delta C_+(t)) + (C_+^* - C_-^*)\delta C_0(t))sin(\Omega t) \end{aligned} \tag{12}$$

Where $Re\{X\}$ and $Im\{X\}$ denote respectively the real and imaginary part of the complex variable X.

In the relation (12) one can see the power variation induced by a small change in the cavity length as a sum of three components

- A continuous component.
- A component in phase at the modulation frequency.
- A component in quadrature at the modulation frequency.

Notice that the continuous part equals zero when the cavity is perfectly resonant regarding to the light frequency, witch means that a small change in the cavity length does not induce a first order variation in the continuous part of the power.

Let $G^0(s)$, $G^+(s)$ and $G^-(s)$ be the transfer functions given by (10) for respectively the carrier and the side-bands. By taking the Laplace transform of (12), one can easily obtain the transfer functions for the in phase and in quadrature part of the power

$$\frac{\delta P_I(s)}{\delta L(s)} = 2Im\{C_0^*(G^-(s) - G^+(s)) + (C_+^* - C_-^*)G^0(s)\} \tag{13}$$

And:

$$\frac{\delta P_Q(s)}{\delta L(s)} = 2Re\{C_0^*(G^-(s) + G^+(s)) + (C_+^* + C_-^*)G^0(s)\} \tag{14}$$

The index I refers to the in phase power component and Q refers to the in quadrature power component. The symbol $(^*)$ denotes the complex conjugate.

3 Interferometer Model

A sketch of the Interferometer considered in this work is given in the figure (2). In order to achieve a maximum sensitivity to gravitational wave the carrier must be resonant in the Fabry-Perot cavities[8] and the interferometer output must be a dark fringe. In order to have an optimal signal to noise ratio both of the carrier and the side-bands must be resonant in the recycling cavity[8, 9, 10, 11]. We assume in this paper that four independent errors signals are extracted from the photodiode D1 (in phase signal), D2 (in phase signal) and D3 (in phase and in quadrature signals).

To achieve the interference conditions four characteristic lengths must be controlled [3]:

- The recycling cavity length: $(l_0 + \frac{l_1+l_2}{2})$.
- The interferometer asymmetry: $\Delta l = (l_1 - l_2)$.
- The Fabry-Perot cavity lengths: L_1 and L_2.

Hence any change of one of these lengths must be sensed in order to maintain the interferometer on its working position. In this section we will give a matrix of transfer functions relating the demodulated current variations to the length variations. The characteristic displacements are given on the figure (3). In order to derive a model for the whole interferometer we will assume that the light propagates instantaneously in the short cavities. This assumption

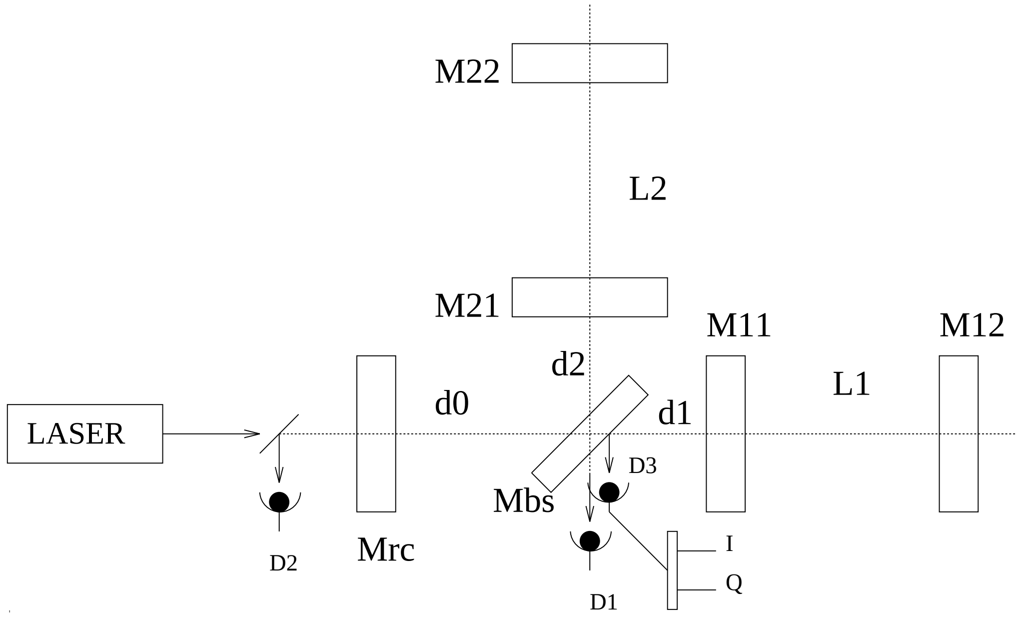

Figure 2: *Interferometer Locking scheme*

is reasonable since the length of the short cavities are very small compared to the Fabry-Perot cavities. This assumption means that we neglect the dynamic effects due to the short cavities.

The model is derived using the following procedure:

1. The fields at any point of the interferometer are computed given the interferometer parameters.

2. The transfer functions for each field variation regarding to the interferometer characteristic lengths are computed using the same procedure as in section (1) with the assumptions given above.

3. The transfer functions for both the in phase and in quadrature power variation are evaluated using the formulas (13) and (14), all these computations are done using Maple package.

Hence using this procedure and considering the signals used for the interferometer locking (fig 2) we can get a transfer function matrix which gives the relation between the four characteristic length variations and the demodulated signals variations[12].

$$\begin{bmatrix} \delta I2_i(s) \\ \delta I1_i(s) \\ \delta I3_i(s) \\ \delta I3_q(s) \end{bmatrix} = M(s) \begin{bmatrix} \delta(l_0 + \frac{l_1+l_2}{2}) \\ \delta(l_1 - l_2) \\ \delta(L_1 + L_2) \\ \delta(L_1 - L_2) \end{bmatrix}$$

The table (1) gives the parameters used for the interferometer transfer functions computation. The transfer function matrix is given in the table (2). The figures (4) to (5) show the

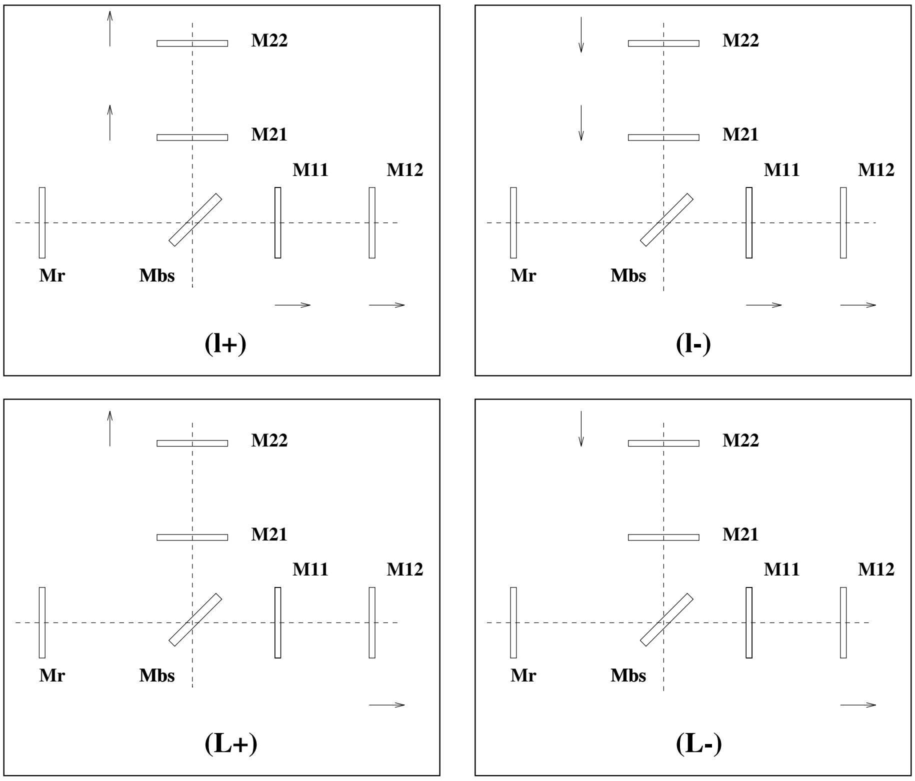

Figure 3: *Interferometer characteristic displacements*

frequential responses corresponding to each element of the matrix $M(s)$.

3.1 Comments

The figures (4) and (5) show that the dynamic effects are important at low frequency, especially when the recycling cavity length changes. Systematic studies have shown that these effects are very dependent on the interferometer parameters. These effects are specially important when the recycling is not optimized i.e. when the recycling miror reflectivity is not chosen in such a way to minimize the light power reflected by the whole interferometer towards the laser.

Let us consider the first plot of the figure (4) which corresponds to the displacement [1] and the in phase signal of the photodiode 2. The corresponding transfer function $M_{11}(s)$ contains two poles at 1.2 kHz and at 3.25 Hz and one zero at approximatively 100 Hz. We will now try to give a physical interpretation of this effect.

The variation of the in phase part of the current given by the diode D1 when we move the recycling miror can be written as the difference of the carrier phase variation and the side-band phase variation:

$$\frac{\delta I}{\delta lr}(s) = K\{\frac{\delta\phi_+}{\delta lr} - \frac{\delta\phi_0}{\delta lr}\} \tag{15}$$

- K is an arbitrary constant.

- δlr refers to the recycling cavity length variation.

Laser Power	P_0=10 Watt
Laser Wave length	λ=1.06μm
Modulation frequency	F_{mod}=6.268428 Mhz
Recycling Mirror:	Reflectivity: R_r=.99; Losses: P_r=0
Fabry-Perot Front Mirror:	Reflectivity: R_1=.85; Losses: P_1=3E-4
Fabry-Perot End Mirror:	Reflectivity: R_2=.9999; Losses: P_2=0
Beam splitter:	Reflectivity: R_s=.5; Losses: P_s=0
Fabry-Perot finesse	$\mathcal{F}_{\mathcal{FP}} \approx 40$
Recycling Factor	≈ 100
Fabry-Perot lengths	L=3km
Recycling cavity and Michelson arms lengths	l0 = 6m l1 = 6.2m l2 = 5.8m

Table 1: *Interferometer Parameters*

	$\delta(l0 + \frac{l1+l2}{2})$	δ(l1 - l2)	δ(L1+L2)	δ(L1-L2)
$\delta I2_i$	$\frac{(4.78e7+.66e5\ S)}{(1+1.3e\text{-}4\ S)\ (1+4.9e\text{-}2\ S)}$	0	$-5.78e8\ \frac{1}{(1+4.9e\text{-}2\ S)}$	0
$\delta I1_i$	0	$-2.51e8\ \frac{1}{(1+2.5e\text{-}4\ S)}$	0	$-6.2e9\ \frac{1}{(1+2.5e\text{-}4\ S)}$
$\delta I3_i$	$\frac{-7.02e5\ \ (1+1.4e\text{-}1\ S)}{(1+1.3e\text{-}4\ S)^2\ (1+4.9e\text{-}2\ S)}$	$2.69e6\ \frac{1}{(1+1.3e\text{-}4\ S)}$	$\frac{-1.67e7}{(1+1.3e\text{-}4\ S)^2\ (1+4.9e\text{-}2\ S)}$	$\frac{-5.71e4}{(1+1.3e\text{-}4\ S)\ \ (1+2.5e\text{-}4\ S)}$
$\delta I3_q$	$\frac{(-3.6e7\text{-}5.02e6\ S)}{(1+1.3e\text{-}4\ S)\ (1+4.9e\text{-}2\ S)}$	$\frac{-5.39e4\ (1+1.5e\text{-}4\ S)\ (1\text{-}1.4e\text{-}3\ S)}{(1+1.3e\text{-}4\ S)^2\ (1+4.9e\text{-}2\ S)}$	$\frac{-8.25e8}{(1+1.3e\text{-}4\ S)\ (1+4.9e\text{-}2\ S)}$	$\frac{-8.3e6}{(1+2.5e\text{-}4\ S)}$

Table 2: *Interferometer Transfer Functions.*

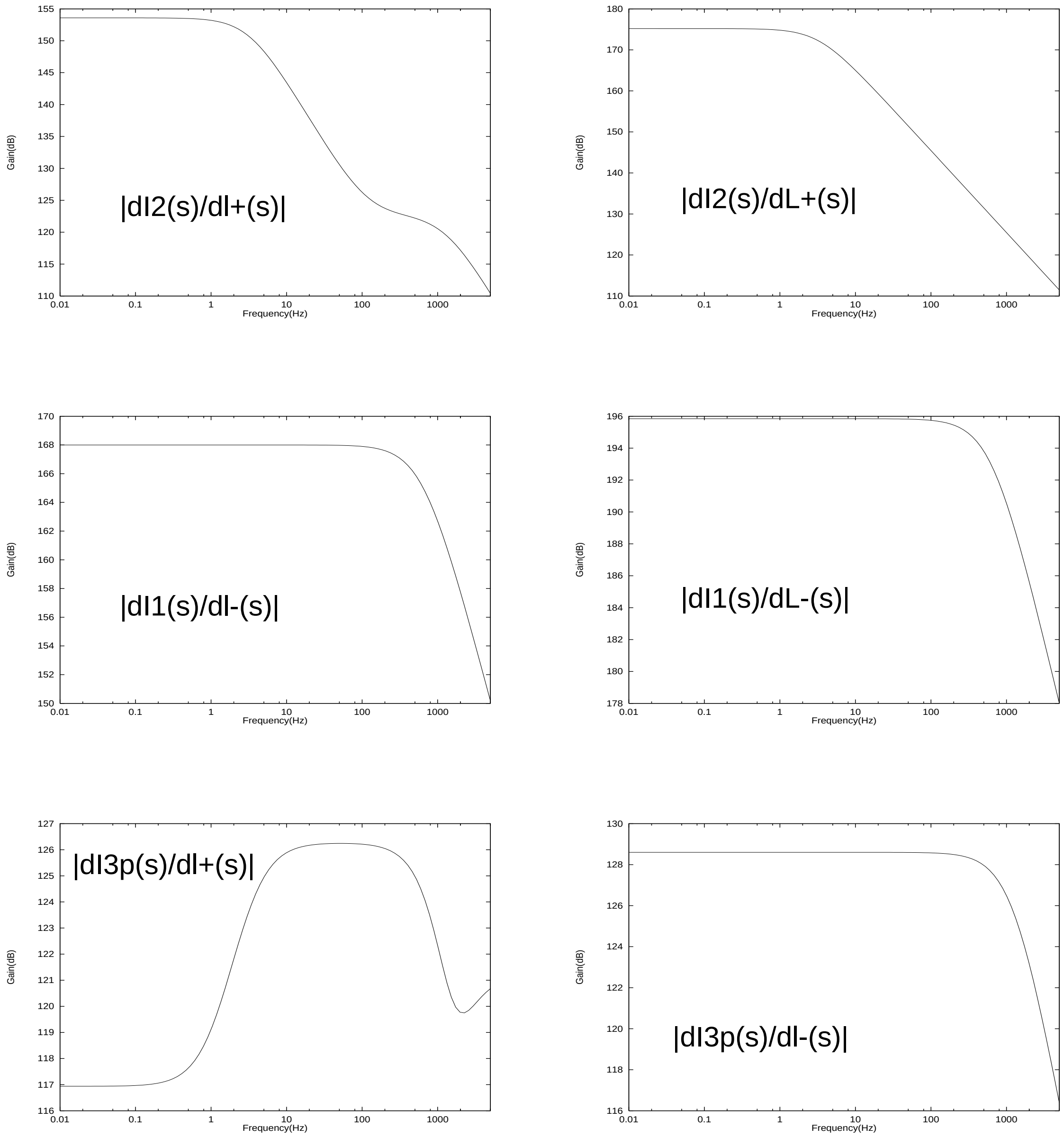

Figure 4: *Interferometer Frequential Responses.*

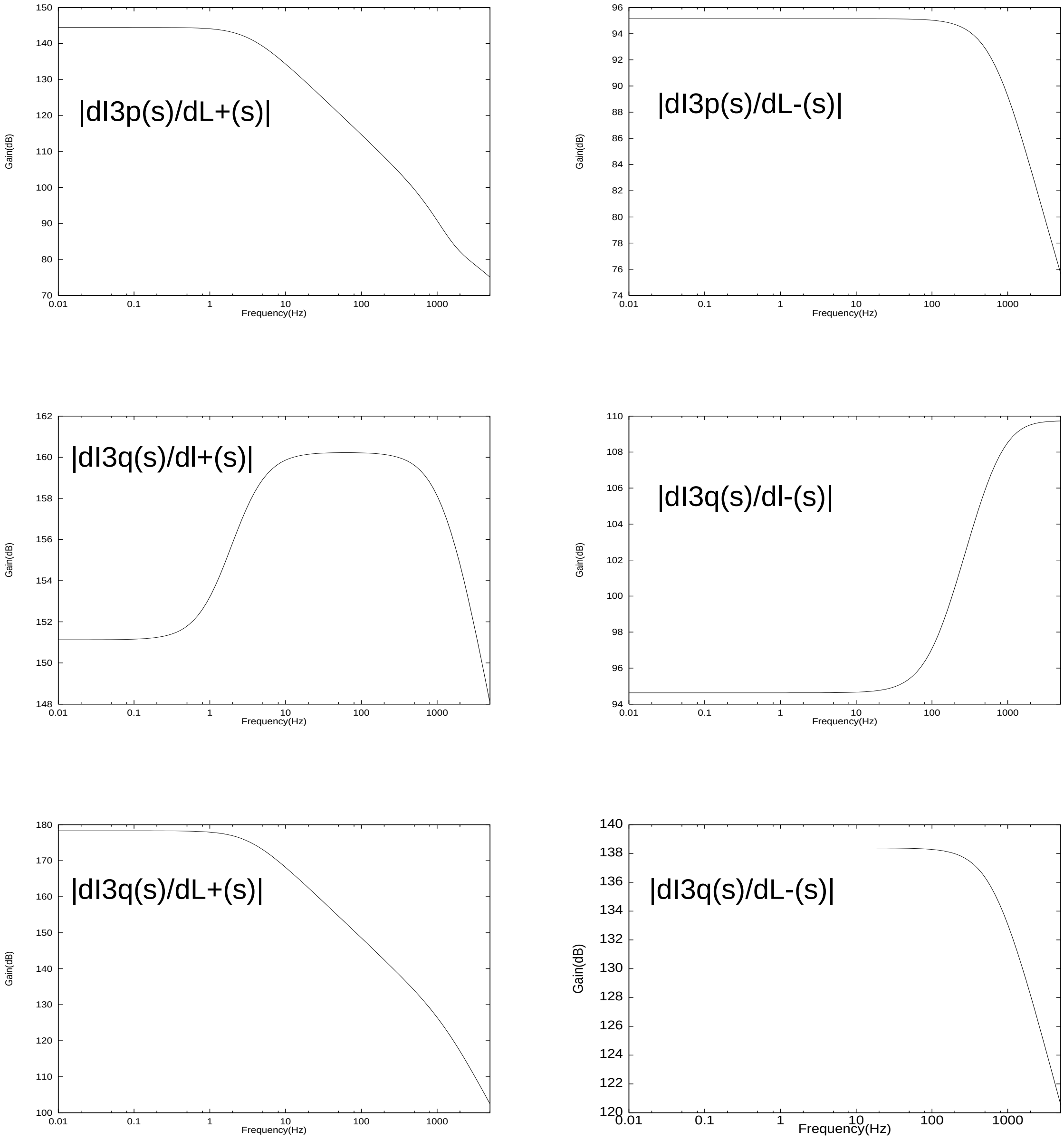

Figure 5: *Interferometer Frequential Responses.*

- $\delta\phi_0$ is the carrier phase variation.
- $\delta\phi_+$ is the side-band phase variation.

One can see the recycling cavity as composed by the recycling mirror and a compound mirror formed by all the others mirrors of the interferometer. Hence we can compute the storage time and the phase variation slope for both the carrier and the side-bands:

$$\tau_r{}^{0,+} = \frac{2}{\pi}\mathcal{F}_r{}^{0,+}(\frac{l_r}{c} + \tau_{FP}{}^{0,+}) \tag{16}$$

In the equation above the indexes '0' and '+' refer respectively to the carrier and the side-band.

- τ_r is the recycling cavity storage time.
- $\mathcal{F}_r$ is the recycling cavity finesse.
- τ_{FP} refers to the Fabry-Perot storage time.
- $l_r = l_0 + \frac{l_1+l_2}{2}$ is the recycling cavity length.

The phase variation slope for the carrier and the side-bands is given by:

$$S_{0,+} = \frac{\Delta\phi_{0,+}}{\Delta l_r} = \frac{-r_c^{0,+}(1-r_r^2)}{(1-r_r r_c^{0,+})(r_r - r_c^{0,+})} \tag{17}$$

- r_r denotes the recycling mirror reflectivity.
- $r_c^{0,+}$ refers to the compound mirror reflectivity for both the carrier and the side-band.

Hence using (15) transfer function for the in phase current is given by:

$$\frac{\delta I}{\delta l_r}(s) = K\{\frac{\Delta\phi_+}{\Delta l_r}\frac{1}{1+\tau_r^+\ s} - \frac{\Delta\phi_0}{\Delta l_r}\frac{1}{1+\tau_r^0\ s}\} \tag{18}$$

The equation above can be written as:

$$\frac{\delta I}{\delta l_r}(s) = K\ \frac{(1+\tau_z\ s)}{(1+\tau_r^+\ s)(1+\tau_r^0\ s)} \tag{19}$$

- $\tau_z = \frac{S_+\tau_r^0 - S_0\tau_r^+}{S_+ - S_0}$
- $K = S_+ - S_0$

The obtained transfer function contains 2 poles corresponding to the carrier and the side-band cut-off frequencies and one zero. Using the parameters of the table (6) leads to:

$$\frac{\delta I}{\delta l_r}(s) = K\ \frac{(1+.0014\ s)}{(1+.0001347\ s)(1+.049\ s)} \tag{20}$$

The transfer function of (20) contains a transmission zero at approximatively 110 Hz and 2 poles respectively at 3 Hz and 1.2 kHz. The poles correspond to the carrier and the side-band cut-off frequencies in the recycling cavity. This result is in accordance with the analytic model derived.

4 Conclusion

We have presented in this paper a frequential model for a large scale interferometer taking into account the filtering effects of the long Fabry-Perot cavities. This model shows some dynamic effects even at low frequency where the interferometer control system will be active. Therefore it is necessary to consider these effects when designing the control system and more especially when extracting the length error signals.

Acknowledgements

The authors whish to thank their colleagues in VIRGO collaboration and especially J.Y.Vinet for useful discussions.

References

[1] A.Abramovici and al. Ligo: The laser interferometer gravitational-wave observatory. *Science*, 256, 1992.

[2] A.Brillet and A.Giazzoto. Virgo conceptual final design, 1994.

[3] R. Flaminio and H.Heitmann. Interferometer locking scheme. VIRGO internal note PJT93021, 1993.

[4] J.Y. Vinet. Virgo meeting. Orsay France, March 1995.

[5] M.Morari and E.Zafiriou. *Robust Process Control*. Prentice-Hall International Editions, 1989.

[6] M.E. Salgado C.E. de Souza and G.C. Goodwin. Issues in time delay modelling. In *IFAC Identification and System, Parameter Estimation, Beijing*, page 549, 1988.

[7] C.Mehmel R.Flaminio and B.Caron. Linear dynamic model for virgo interferometer. VIRGO internal note NTS95039, 1995.

[8] R.W.P Drever. Interferometric detectors for gravitational radiation. In *Gravitational Radiation*, page 321. N.Deruelle and T.Piran eds, North-Holland, Amsterdam, 1983.

[9] C.N.Man J-Y.Vinet, B.Meers and A.Brillet. Optimization of long-baseline optical interferometers for gravitational-wave detection. *Physical Review D*, 38(2):433, 1988.

[10] D.Shoemaker P.Fritschel and R.Weiss. Demonstration of light recycling in a michelson interferometer with fabry-perot cavities. *Applied Optics*, 31(10):1412, 1992.

[11] C.N.Man. Frontal modulation of an interferometer with recycling. VIRGO internal note PJT 92033a, 1992.

[12] C.Mehmel and Al. Interferometer transfer functions. VIRGO internal note NTS96004, 1996.